Capture Point Trajectories for Reduced Knee Bend using Step Time Optimization

Robert J. Griffin[1,2], Sylvain Bertrand[1], Georg Wiedebach[1], Alexander Leonessa[2], Jerry Pratt[1]

Abstract— Traditional force-controlled bipedal walking utilizes highly bent knees, resulting in high torques as well as inefficient, and unnatural motions. Even with advanced planning of center of mass height trajectories, significant amounts of knee-bend can be required due to arbitrarily chosen step timing. In this work, we present a method that examines the effects of adjusting the step timing to produce plans that only require a specified amount of knee bend to execute. We define a quadratic program that optimizes the step timings and is executed using a simple iterative feedback approach to account for higher order terms. We then illustrate the effectiveness of this algorithm by comparing the walking gait of the simulated Atlas humanoid with and without the algorithm, showing that the algorithm significantly reduces the required knee bend for execution. We aim to later use this approach to achieve natural, efficient walking motions on humanoid robot platforms.

I. INTRODUCTION

Humanoid robots have been demonstrated capable of robustly walking across flat surfaces, recovering from pushes and uncertainties, and walking across varying terrain. They are also demonstrating increasingly dynamic behavior when walking, a major step forward from the slow, quasi-static walking that was previously standard. However, while there are some exceptions, most all of the gaits employed feature highly bent knees, walking with an almost "squatted" motion. This is highly unnatural, and, while it offers some control benefits, results in significant increases in power consumptions of the knee [1] over that seen in humans [2]. It additionally decreases ground clearance of the robot and creates clearance issues when walking over varied terrain.

Before tackling the host of control challenges introduced by walking with straighter legs, the underlying dynamic plans used by the robot must be conducive to walking with less-bent knees. While whole-body planning schemes that consider the full rigid-body dynamics of the robot have made significant improvements in speed, they typically require too long of solve times for online implementation. Instead, a typical approach for dealing with the highly nonlinear and high dimensional problem of planning and controls for humanoids is to restrict consideration to the center of mass (CoM). These low-order dynamic representations have been often preferred for online implementation due to their speed and efficiency. The zero-moment point (ZMP) is an often utilized
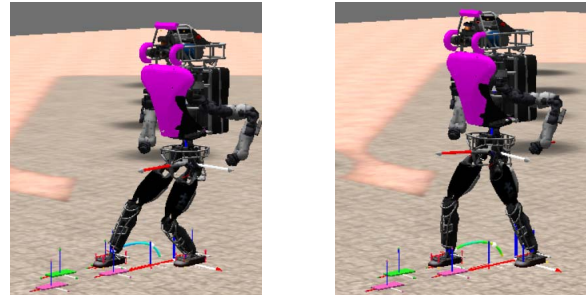

Fig. 1. Without considering the effects of step timing, ICP plans can require significant knee-bend to execute (left). Modifying the timing, however, can result in dynamic, natural, and efficient dynamic plans (right).

representation of the CoM dynamics, and is the point on the ground plane where the moment induced by the inertial and gravitational force is perpendicular to the surface [3], It has been used to generate stable walking motions that avoid tipping about the foot edges of the robot [1], [4], [5]. Alternatively, the instantaneous capture point (ICP) [6] and divergent component of motion (DCM) [7] were introduced as stable state transformations of the CoM, and have been shown as highly effective strategies for momentum-based planning and control of humanoid robots [8], [9].

Several works have attempted to address planning and control of appropriate height trajectories for straighter legs. In [10], the authors presented an approach for generating straightened-knee trajectories by combining model predictive control (MPC) of the ZMP to generate horizontal CoM trajectories with a spring-damper approach to generate vertical CoM trajectories. Alternatively, [11] used linear differential inclusion to incorporate these height trajectories directly into the MPC, resulting in relatively natural, cyclical motions of the CoM. In [12], the authors also included CoM height in their ZMP-based quadratic program, but required sequential quadratic programming to solve the resulting problem's quadratic constraints. The planning and control of height trajectories as they affect the DCM was addressed in [9], which relaxed the assumption of a constant pendulum height in an attempt to increase control of the CoM height over variable terrain. This last is an example of the standard planning approach, as noted by [11], with CoM height planning typically done independently of horizontal planning, leaving planners ill-equipped to deal with kinematic limitations. This issue comes to the forefront when attempting to walk with straighter legs.

While some previous works are capable of generating kinematically feasible height trajectories [10], [11], these approaches, along with most others, typically rely on arbitrarily chosen single and double support phase durations. While

kinematic feasibility of the CoM height plan is guaranteed, this has the fundamental limitation of ignoring the effects of step timing on the resulting horizontal CoM plans. This is, in turn, ignoring the kinematic constraints placed on the system by the timing and the dynamic plan, potentially requiring significant knee-bend during execution. As the walking speed of most humanoid robot platforms is still relatively slow, this becomes common, with the robot needing to crouch for the next step to be kinematically feasible, as shown on the left of Figure 1. As the step length increases, the required knee-bend of this slow step correspondingly increases, as well. To address this, we present in this work an approach for optimizing the swing and transfer durations to produce ICP trajectories that do not require knee-bend beyond an amount specifiable by the operator. We utilize a novel quadratic program that uses the gradient of the ICP plan w.r.t. to time to compute the required timing adjustments that satisfy the desired maximum and minimum knee-bend kinematic constraints. We believe that proper timing selection is critical to the continued progress of humanoid locomotion towards efficient, human-like gaits.

II. DYNAMIC PLANNING BACKGROUND

An increasingly common approach for dynamic planning in humanoid robots is to utilize a stable transformation of the CoM position and velocity in the form of either the ICP, DCM, or extrapolated center of mass (XCoM) [6]–[9], [13]–[16]. In this work, we will refer only to the ICP, noting its equivalency to the DCM and XCoM in the x-y plane. The ICP is, as mentioned, a stable transformation of the CoM state, and is defined as

$$\boldsymbol{\xi} = \mathbf{x} + \frac{1}{\omega}\dot{\mathbf{x}}, \tag{1}$$

where $\boldsymbol{\xi}$ is the ICP position, $\mathbf{x}$ and $\dot{\mathbf{x}}$ are the CoM position and velocity, and $\omega = \sqrt{g/\Delta z_{\text{com}}}$ is the natural frequency of the inverted pendulum. By reordering this, we can see that the CoM has stable first order dynamics with respect to the ICP, meaning that it will converge to the ICP over time. Through differentiation, the ICP dynamics are defined as

$$\dot{\boldsymbol{\xi}} = \omega\left(\boldsymbol{\xi} - \mathbf{r}_{\text{cmp}}\right), \tag{2}$$

where we see that the Centroidal Moment Pivot (CMP) point [17], $\mathbf{r}_{\text{cmp}}$, controls the ICP dynamics.

A. Dynamic Planning of ICP Trajectories

There are a variety of methods that have been used to generate stable ICP trajectories, such as [9], where discrete trajectories were generated numerically from specified ZMP trajectories. In this work, we use the algorithm proposed in [8], summarized in the following paragraphs.

From the definition of the ICP dynamics in Equation 2, the differential equation has an analytic solution

$$\boldsymbol{\xi}(t) = e^{\omega t}\left(\boldsymbol{\xi}_0 - \mathbf{r}_{\text{cmp}}\right) + \mathbf{r}_{\text{cmp}}, \tag{3}$$

assuming $\mathbf{r}_{\text{cmp}}$ is held constant. Using this, we can calculate a desired ICP trajectory for walking, given a set of desired footsteps and desired CMP locations in those footsteps. To
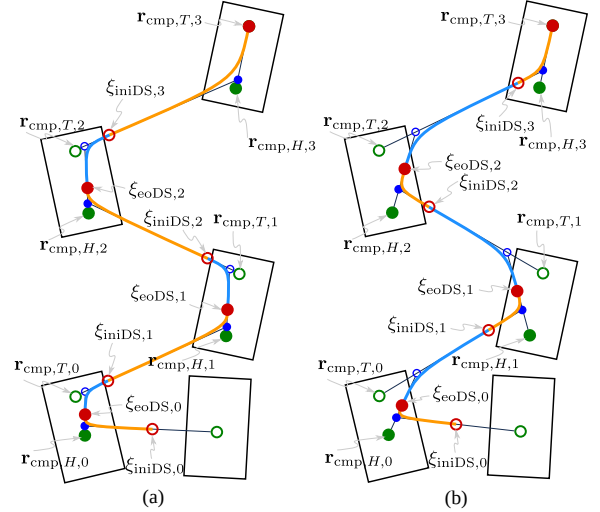

Fig. 2. Heel-to-Toe ICP trajectory with smooth CMP trajectories for slower (left) and faster (right) steps [8].

more accurately represent human-like walking, we use two CMPs per foot, one in the heel ($\mathbf{r}_{\text{cmp},H}$) and one in the toe ($\mathbf{r}_{\text{cmp},T}$), as shown in Figure 2 by the green circles. This results in the reference CMP trajectory moving from the heel to the toe in the foot while stepping.

To determine the amount of time spent on the CMP, we can break the ICP plan into four segments, $T_{\text{iniDS}}, T_{\text{endDS}}, T_{\text{iniSS}}$, and T_{endSS}. These correspond roughly to the time in transfer shifting the weight to the upcoming support foot, the time in transfer shifting the weight forward in the foot, the time in swing shifting the weight forward in the foot, and the time spent in swing with the weight in the front of the foot, respectively. The desired ICP trajectory can be calculated by recursing backward from the final objective location. This can be done by using the solution to the ICP dynamics in Equation 3, and assuming a static CMP location, allowing the ICP locations to be computed at the beginning and end of swing and transfer. We can smooth the ICP trajectories using third order polynomial interpolation between each of these points, which guarantees smoothness of the CMP trajectory [8], resulting in the light blue and orange colored lines in Figure 2.

Note that the effect of taking slower steps is highlighted in Figure 2. This results in much more of the ICP motion occurring during transfer. This, in turn, has great effects on the location of the CoM when walking.

B. Computation of CoM Trajectory Solutions

While the utilization of the ICP for dynamic planning has the major advantage of not requiring specific calculation of CoM trajectories, this is required for determination of kinematic feasibility. In particular, we want to know the location of the CoM at touchdown, as this is the farthest point from both the leading and trailing feet. By using the ICP algorithm in [8], we can obtain an analytic solution for the CoM trajectory. If the ICP trajectory is defined using a constant CMP, as in Equation 3, the CoM trajectory can be
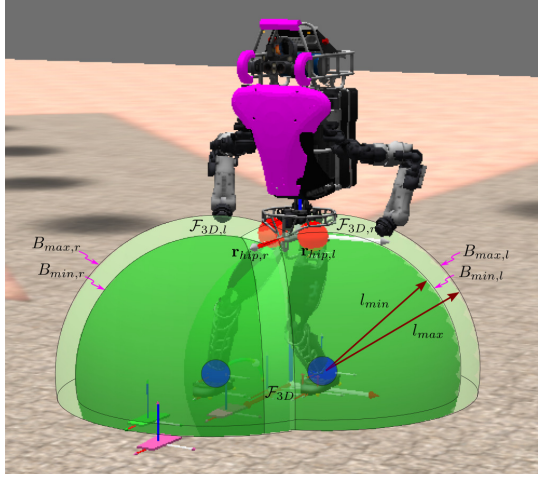
Fig. 3. Illustration of the kinematic constraints we are using to calculate the desired CoM adjustments. The light green spheres represent the area in which the hips (the red dots) must be located to be reachable with the legs at maximum extension. The dark green spheres represent the area outside of which the hips must be located to guarantee bending less than some specifiable amount.

defined by integrating the CoM dynamics

$$\dot{\mathbf{x}}(t) = \omega \left(e^{\omega t} \left(\boldsymbol{\xi}_0 - \mathbf{r}_{\text{cmp}} \right) + \mathbf{r}_{\text{cmp}} - \mathbf{x}(t) \right), \qquad (4)$$

which has the solution

$$\mathbf{x}(t) = \tfrac{1}{2} e^{\omega t} \left(\boldsymbol{\xi}_0 - \mathbf{r}_{\text{cmp}} \right) - \tfrac{1}{2} e^{-\omega t} \left(\boldsymbol{\xi}_0 + \mathbf{r}_{\text{cmp}} - 2\mathbf{x}_0 \right) + \mathbf{r}_{\text{cmp}}. \qquad (5)$$

Alternatively, if the ICP trajectory is defined using a cubic polynomial, the CoM dynamics become

$$\dot{\mathbf{x}}(t) = \omega \left(\mathbf{c}_0 + \mathbf{c}_1 t + \mathbf{c}_2 t^2 + \mathbf{c}_3 t^3 - \mathbf{x}(t) \right), \qquad (6)$$

which has the solution

$$\begin{aligned}
\mathbf{x}(t) = & \mathbf{c}_3 t^3 + \left(\mathbf{c}_2 - \tfrac{3}{\omega} \mathbf{c}_3 \right) t^2 + \left(\mathbf{c}_1 - \tfrac{2}{\omega} \mathbf{c}_2 + \tfrac{6}{\omega^2} \mathbf{c}_3 \right) t \\
& + \left(\mathbf{c}_0 - \tfrac{1}{\omega} \mathbf{c}_1 + \tfrac{2}{\omega^2} \mathbf{c}_2 - \tfrac{6}{\omega^3} \mathbf{c}_3 \right) \\
& + e^{-\omega t} \left(\mathbf{x}_0 - \mathbf{c}_0 + \tfrac{1}{\omega} \mathbf{c}_1 - \tfrac{2}{\omega^2} \mathbf{c}_2 + \tfrac{6}{\omega^3} \mathbf{c}_3 \right).
\end{aligned} \qquad (7)$$

Using these equations, we can then calculate where the CoM will be located at touchdown.

III. CENTER OF MASS ADJUSTMENT CALCULATION

Before we can calculate the desired timing adjustments in the ICP plan, we must determine *how* we want to adjust the plan itself. To do this, we can determine the requirements placed on the CoM location that satisfy our kinematic constraints placed on the system; namely that of maximum and minimum leg extension. We can use these constraints to define the "feasibility region" for the CoM as the area where the CoM can be located so that both legs do not bend more or less than desired.

To compute the three dimensional feasibility region, we can observe that placing limits on the amount of knee bend at both full retraction and full extension acts to constrain the location of the robot's hips. We can calculate these areas exactly by defining a series of spheres whose radius is a function of the retracted (when it is most bent) and extended (when it is least bent) leg length. By defining a maximum and

minimum amount of leg bend, $\theta_{\max}$ and $\theta_{\min}$, respectively, we can calculate the corresponding bent and extended leg length, l_{min} and l_{max}. We can then use this to define a sphere centered at the ankle, $B_{\min}$ that the hip joint must be located outside of, shown by the dark green spheres in Figure 3. In doing so, we then know that as long as, at touchdown, both hip joints are located outside of these spheres, the ICP plan will not require either knee to bend past $\theta_{\max}$. Additionally, a second set of spheres can be defined, $B_{\max}$, shown by the lighter green spheres in Figure 3, to constrain the hip locations to be achievable at full leg extension.

Using these concentric set of spheres, we can compute the 3D feasibility region, $\mathcal{F}_{3D} \subset \mathbb{R}^3$, to constrain the CoM location by saying the hip locations must be within $B_{\max}$ and outside of $B_{\min}$, or

$$\mathbf{r}_{\text{hip}} \in \mathcal{F}_{3D} \equiv \{ B_{\max} - B_{\min} \} \subset \mathbb{R}^3, \qquad (8)$$

which is illustrated in Figure 3. Here, the ankle locations are the blue balls, while the hip locations of the robot are the red balls. As can be seen, if both hips are located inside the sphere of the maximum leg length and outside the sphere of the minimum leg length at touchdown, the plan is both kinematically achievable and will not require bending either knee past $\theta_{\max}$.

From the 3D feasible space, we can compute the 2D feasibility region, $\mathcal{F}_{2D} \subset \mathbb{R}^2$, in the x-y plane where the CoM must be located, shown as the shaded green region in Figure 4. To do so, we assume that the distance from the CoM to each hip can be treated as a constant, a fairly common [10] and accurate assumption due to the mass distribution on most humanoid robots. This allows us to offset the sphere origins from the ankle locations, defining the blue circles in Figure 4 as $\mathbf{s}_l$ and $\mathbf{s}_r$, enabling us to directly consider the CoM rather than the hip locations as in Figure 3. $\mathcal{F}_{2D}$ then becomes much simpler to calculate, being bounded on the sides by straight lines perpendicular to the vector from one ankle to the other when walking with constant ankle height,

$$F_{\min} \perp \overrightarrow{\mathbf{s}_{l,r}}, \qquad F_{\max} \perp \overrightarrow{\mathbf{s}_{l,r}}. \qquad (9)$$

This follows directly from projecting $\mathcal{F}_{3D}$ in Equation 8 onto the x-y plane. This approach extends to non-flat ground by using arcs instead of lines.

The objective then becomes to compute the distance required to project the CoM into the feasibility region,

$$\Delta x_\parallel = \mathrm{d}\left(\mathbf{x}, \mathcal{F}_{2D} \right). \qquad (10)$$

We can simplify this adjustment as being along the vector $\overrightarrow{\mathbf{s}_{l,r}}$, the red line in Figure 4. From the definition of the bounds of the set in Equation 9, this is equivalent to

$$\Delta x_\parallel = \begin{cases} \mathrm{d}(\mathbf{x}, F_{\max}), & x > f_{\max}, \\ 0, & f_{\min} \leq \mathbf{x} \leq f_{\max}, \\ \mathrm{d}(\mathbf{x}, F_{\min}), & x < f_{\min}, \end{cases} \qquad (11)$$

where $f_{\max}$ and $f_{\min}$ are the points where $\overrightarrow{\mathbf{s}_{l,r}}$ intersections $F_{\max}$ and $F_{\min}$, respectively. This provides the desired CoM

Fig. 4. Illustration of the approach for computing the desired CoM adjustment. The region where the CoM is both kinematically feasible and satisfies the max knee bend is represented by the shaded green area. The desired CoM adjustment is the distance from CoM to the feasibility region.

adjustment of ICP plan to achieve the desired kinematic motions.

IV. TIMING OPTIMIZATION ALGORITHM

Now that we can compute the desired CoM adjustment, we must develop a tool for modifying the ICP plan to achieve this adjustment. The CoM trajectory is a function of the CMP position and step timing. As the CMP position is defined according to the step plan, it can be assumed fixed, requiring the durations used in the ICP plan to be modified to achieve the necessary CoM adjustment. The objective CoM adjustment can be found by computing the CoM location at touchdown, $\mathbf{x}_f$, at the beginning of each step through integrating the dynamic plan. Using the planning algorithm in section II, this can be done with the analytic solutions in Equation 5 and Equation 7, although it can be found using numerical integration for any ICP plan, as well. Then, using $\mathbf{x}_f$, we can compute the objective parallel adjustment $\Delta x_\parallel$ using the approach outlined in section III. The ICP plan however, is a function of several timing elements, meaning the timing adjustments cannot be explicitly solved for from only the desired CoM adjustment, as the problem is under-constrained. Instead, we can cast the problem in an optimization framework, defining additional cost objectives to calculate an optimal set of timing adjustments. We will do so in the following section by defining a quadratic program (QP) with an iterative feedback loop.

From the definition of the ICP plan in section II, we can define the step timing variables to be used in the adjustment calculation as

$$\mathbf{T} = \begin{bmatrix} T_{\text{iniDS},0} & T_{\text{endDS},0} & T_{\text{iniSS},0} & \cdots \\ T_{\text{endSS},0} & T_{\text{iniDS},1} & T_{\text{endDS},1} \end{bmatrix}^T, \quad (12)$$

where the subscript number indicates the associate step, with 0 being current. While these variables are specific to the ICP planning approach presented in [8], variables for other ICP planning approaches can be equivalently defined. Due to the definition of the ICP dynamics, however, the ICP and resulting CoM plans are highly nonlinear with respect to

time, where the CoM location at touchdown can be defined as some nonlinear function,

$$\mathbf{x}_f = \mathbf{f}(\mathbf{T}). \quad (13)$$

A method of determining the optimal durations, $\mathbf{T}^*$ is required. While nonlinear optimization is possible, we prefer to use a QP due to its reliability and efficiency. To do so, we can approximate the gradients of $\mathbf{f}(\cdot)$ with respect to $\mathbf{T}$,

$$\nabla_{\mathbf{T}}\mathbf{f} = \begin{bmatrix} \nabla\mathbf{f}_{T_{\text{iniDS},0}} & \nabla\mathbf{f}_{T_{\text{endDS},0}} & \nabla\mathbf{f}_{T_{\text{iniSS},0}} & \cdots \\ \nabla\mathbf{f}_{T_{\text{endSS},0}} & \nabla\mathbf{f}_{T_{\text{iniDS},1}} & \nabla\mathbf{f}_{T_{\text{endDS},1}} \end{bmatrix}, \quad (14)$$

by slightly perturbing the function $\mathbf{f}(\cdot)$ such that

$$\delta\mathbf{x}_f = \nabla_{\mathbf{T}}\mathbf{f}\delta\mathbf{T} + \text{H.O.T.}. \quad (15)$$

The gradient function in Equation 14 can be broken into components parallel and perpendicular to the desired CoM adjustment, $\nabla f_\parallel(\mathbf{T})$ and $\nabla f_\perp(\mathbf{T})$, respectively. This then allows us to define a QP using $\nabla_{\mathbf{T}}\mathbf{f}(\mathbf{T})$.

We can describe the desired CoM adjustment as a quadratic objective function of the step durations,

$$J_\parallel = \left\| \Delta x_\parallel - \nabla f_\parallel \Delta\mathbf{T} \right\|_{Q_\parallel}^2. \quad (16)$$

We prefer to define this as an objective instead of an equality constraint, as this formulation prevents the problem from being over-constrained if limits are placed on $\Delta\mathbf{T}$. We can then define additional quadratic objective function, such as the minimization of perpendicular CoM adjustments,

$$J_\perp = \left\| \nabla f_\perp \Delta\mathbf{T} \right\|_{Q_\perp}^2, \quad (17)$$

and the minimization of the total timing adjustment,

$$J_T = \left\| \Delta\mathbf{T} \right\|_{\mathbf{R}_T}^2. \quad (18)$$

Lastly, we can define a cost function to minimize the timing symmetry between the duration of the beginning of each walking phase, $T_{\text{ini},i}$, and the end of each walking phase, $T_{\text{end},i}$,

$$J_\alpha = \left\| \Delta\mathbf{T}_{\text{ini}} - \Delta\mathbf{T}_{\text{end}}, \right\|_{R_\alpha}^2, \quad (19)$$

which yields ICP plans with more desirable CMP trajectories when using the planning approach from [8]. The total cost function is then defined as

$$J = J_\parallel + J_\perp + J_T + J_\alpha, \quad (20)$$

with a corresponding optimal solution

$$\Delta\mathbf{T}^* = \text{argmin } J(\Delta x_\parallel, \Delta\mathbf{T}). \quad (21)$$

However, as this algorithm ignores the higher order terms in Equation 15, the resulting CoM adjustment from $\Delta\mathbf{T}^*$ are not likely to be equivalent to the desired adjustment, $x_\parallel \neq f_\parallel(\mathbf{T} + \Delta\mathbf{T}^*)$. This means that the QP is not likely to find an adjustment satisfying the kinematic constraints on the first iteration. To compensate for this, we can, similar to Sequential Quadratic Programming, define an iterative feedback-based loop

$$\Delta x_\parallel^{i+1} = \Delta x_\parallel^i + k_p e_\parallel, \quad (22)$$

(1a) (1b) (1c) (1d) (1e) (1f)
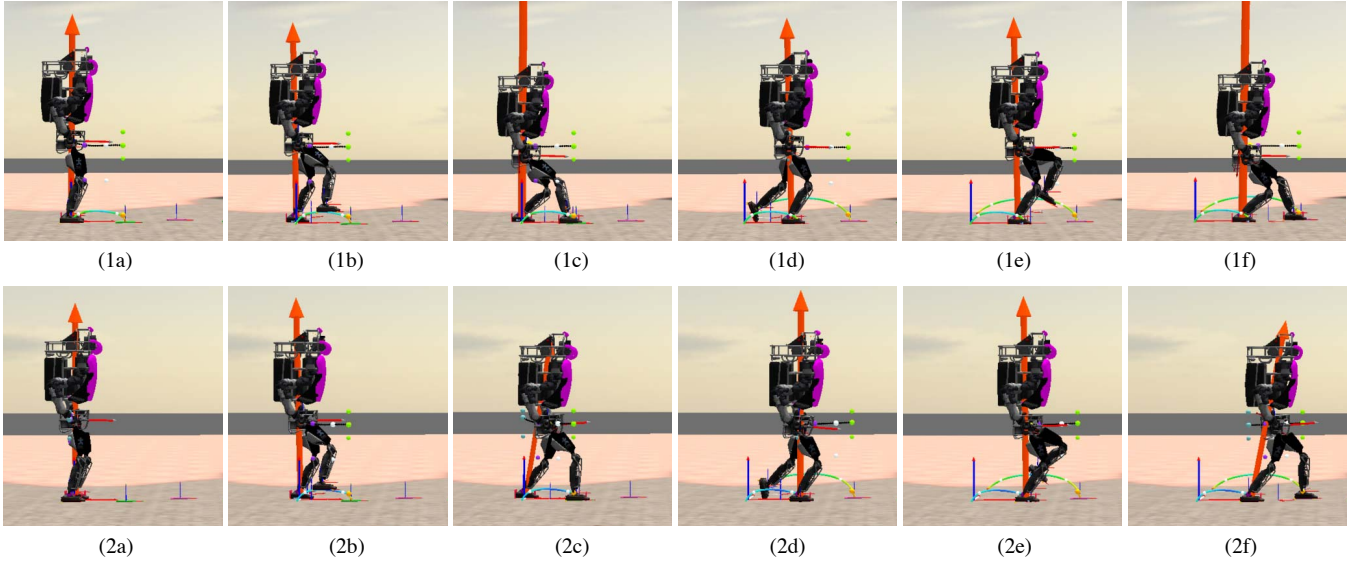
(2a) (2b) (2c) (2d) (2e) (2f)

Fig. 5. Comparison between walking without the time optimization module active (top) and with the time optimization module active (bottom). The desired steps are 0.6m long, using a 2.5s swing and 2.5s transfer. In this case, the maximum desired knee bend is 0.4 rads, and the resulting total step duration is reduced.
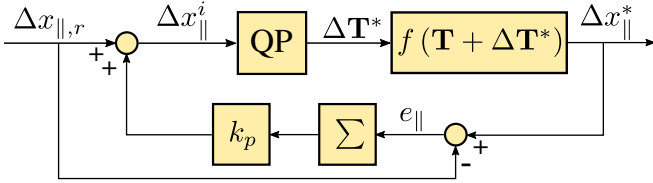

Fig. 6. Block diagram of the feedback loop for calculating the timing adjustment. The loop is performed until the desired adjustment is achieved, with a feedback based on the achieved adjustment in each iteration.

where $e_\parallel = \Delta x_{\parallel,r} - \Delta x_\parallel^*$ is the error between the achieved adjustment using the QP solution and the original desired CoM adjustment, $\Delta x_\parallel^i$ is the desired adjustment used in the current solver iteration, and $\Delta x_\parallel^{i+1}$ is the desired adjustment for the next iteration. This feedback loop is repeated until the error $e_\parallel$ is less than a fixed amount, $|e_\parallel| < \epsilon$, at which the loop is terminated. At the end of each iteration, the objective adjustment for next iteration, $\Delta x_\parallel^{i+1}$, is computed. The loop can also be terminated once a specified maximum number of iterations is exceeded.

V. RESULTS

The algorithm was implemented in the IHMC Open Source Software system, using the Simulation Construction Set. To solve the QP, a custom implementation of the Goldfarb-Idnani solver was used. Balance is controlled when simulating the Atlas humanoid using the momentum-based whole-body controller outlined in [18].

A simulation of walking using 5.0s, 0.6m steps with and without using this algorithm is shown in Figure 5. As can be seen in the top row, specifically panels 1c and 1f, using the fixed provided timing without adjustment requires significant bending of the knee for the step to be reached. The bottom row illustrates walking using the presented algorithm. The step durations are modified to require only 0.4rad of knee-bend, producing a much more natural, dynamic gait. The reduction in knee bend can be seen when comparing with

panels 2c and 2f. The necessary timing adjustments are shown in Figure 7, and are discussed in detail later.

The resulting timing adjustments calculated using the algorithm for three different step lengths to achieve different degrees of knee bend are shown in Figure 7. Here, we compare the timing adjustment results for relatively slow steps, a 2.5s swing duration and 2.5s transfer duration when allowing a differing degree of knee-bend. For short (0.2m) steps, the motion results in approximately 0.45rad of bend at the knee using the original, slow 5.0s step duration. If we specify that we would like the legs to be straighter, i.e. less knee-bend, the transfer duration of the upcoming step is decreased until the knees are only bent by the specified amount, while the other durations are unchanged. The optimization prefers to use the upcoming transfer duration, as it is the most effective means to adjust the CoM position, as illustrated in Figure 2.

For medium length (0.4m) steps, as shown in the middle plot of Figure 7, the step requires significantly more knee-bend at the original 5s duration than the short step length, needing approximately 0.8rad of bend. The optimization again primarily utilizes the upcoming transfer duration. As we placed constraints on the minimum durations for the different transfer segments, however, the current swing duration is also somewhat adjusted in the most extreme cases, as this offers slight modifications of the CoM positions.

For longer (0.6m) steps, as shown in the bottom plot of Figure 7, the user specified step duration of 5s requires a large amount of knee-bend, greater than 1.2rad. By trying to minimize knee bend, the upcoming transfer duration is made as small as possible. The current swing duration is also increased as the maximum knee bend is decreased in an attempt to achieve the desired amount of CoM adjustment.

It is worth noting that, for all step lengths, the current transfer duration has virtually no effect on the final CoM position when using the ICP planner outlined in [8]. Additionally, in practical implementation, allowing the current swing duration to increase provides relatively little benefit,
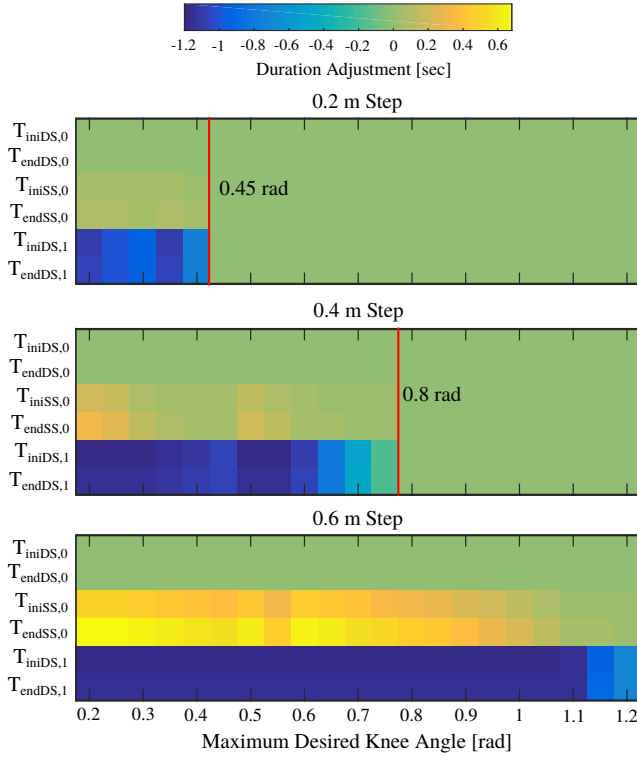
Fig. 7. Timing adjustments while taking 0.2m, 0.4m, and 0.6m steps and 5s pre-adjusted step durations.

with almost all effective adjustments coming from the upcoming transfer duration.

VI. Conclusion

Using the presented approach, we were able to modify existing ICP plans to produce walking gaits that require minimal knee bend. Traditional walking approaches utilize highly bent knees, which has been somewhat addressed in other works by attempting to straighten the legs to their maximum feasible length while walking. This, however, overlooks the kinematic constraints that fixed step timing places on the CoM height and corresponding knee angles. This work represents, to our knowledge, the first study of the effects of the step duration in the resulting dynamic plans and their corresponding CoM heights.

We presented an approach that utilizes a quadratic program optimization scheme to compute the necessary step timing adjustments to produce plans that require a specified amount of knee bend, while remaining kinematically feasible. This algorithm is then illustrated to successfully adjust the ICP plan timing to reduce the knee bend to the desired angle. As robots move towards walking with straighter legs and more natural, efficient gaits, the effects of step timing will become increasingly important, with this work representing a critical first step towards achieving these motions.

In future work, we plan to utilize this algorithm along with advanced CoM height control techniques to enable humanoid robots to efficiently walk with straight legs using momentum-based whole-body control frameworks. We also plan to extend this work to account for kinematic effects of toe-off and pelvis orientation changes on reachability.

References

[1] S. Kajita, F. Kanehiro, K. Kaneko, K. Fujiwara, K. Harada, K. Yokoi, and H. Hirukawa, "Biped walking pattern generation by using preview control of zero-moment point", in *IEEE International Conference on Robotics and Automation (ICRA)*, 2003, pp. 1620–1626.

[2] D. A. Winter, *Biomechanics and motor control of human movement*. John Wiley & Sons, 2009.

[3] P. Sardain and G. Bessonnet, "Forces acting on a biped robot. Center of Pressure-Zero Moment Point", *IEEE Transactions on Systems, Man and Cybernetics, Part A: Systems and Humans*, vol. 34, no. 5, pp. 630–637, Sep. 2004.

[4] K. Harada, S. Kajita, K. Kaneko, and H. Hirukawa, "An analytical method for real-time gait planning for humanoid robots", *International Journal of Humanoid Robotics*, vol. 3, no. 01, pp. 1–19, 2006.

[5] P.-B. Wieber, "Trajectory free linear model predictive control for stable walking in the presence of strong perturbations", in *6th IEEE-RAS International Conference on Humanoid Robots (Humanoids)*, Genova, Italy, Dec. 2006, pp. 137–142.

[6] J. Pratt, J. Carff, S. Drakunov, and A. Goswami, "Capture Point: A Step toward Humanoid Push Recovery", in *6th IEEE-RAS International Conference on Humanoid Robots (Humanoids)*, Dec. 2006, pp. 200–207.

[7] T. Takenaka, T. Matsumoto, and T. Yoshiike, "Real time motion generation and control for biped robot -1st report: Walking gait pattern generation", in *IEEE/RSJ International Conference on Intelligent Robots and Systems (IROS)*, Oct. 2009, pp. 1084–1091.

[8] J. Englsberger, T. Koolen, S. Bertrand, J. Pratt, C. Ott, and A. Albu-Schäffer, "Trajectory generation for continuous leg forces during double support and heel-to-toe shift based on divergent component of motion", in *IEEE/RSJ International Conference on Intelligent Robots and Systems (IROS)*, Sep. 2014, pp. 4022–4029.

[9] M. A. Hopkins, D. W. Hong, and A. Leonessa, "Humanoid locomotion on uneven terrain using the time-varying Divergent Component of Motion", in *2014 IEEE-RAS International Conference on Humanoid Robots*, Nov. 2014, pp. 266–272.

[10] Z. Li, N. G. Tsagarikis, D. G. Caldwell, and B. Vanderborght, "Trajectory generation of straightened knee walking for humanoid robot iCub", in *11th International Conference on Control, Automation, Robotics and Vision, ICARCV 2010*, 2010, pp. 2355–2360.

[11] C. Brasseur, A. Sherikov, C. Collette, D. Dimitrov, and P.-B. Wieber, "A robust linear MPC approach to online generation of 3d biped walking motion", in *15th IEEE-RAS International Conference on Humanoid Robots (Humanoids)*, Nov. 2015, pp. 595–601.

[12] K. Van Heerden, "Planning COM trajectory with variable height and foot position with reactive stepping for humanoid robots", in *Robotics and Automation (ICRA), 2015 IEEE International Conference on*, 2015, pp. 6275–6280.

[13] J. E. Pratt, T. Koolen, T. De Boer, J. Rebula, S. Cotton, J. Carff, M. Johnson, and P. Neuhaus, "Capturability-based analysis and control of legged locomotion, part 2: Application to M2V2, a lower body humanoid", *The International Journal of Robotics Research*, vol. 31, no. 10, pp. 1117–1133, 2012.

[14] M. Morisawa, S. Kajita, F. Kanehiro, K. Kaneko, K. Miura, and K. Yokoi, "Balance control based on Capture Point error compensation for biped walking on uneven terrain", in *12th IEEE-RAS International Conference on Humanoid Robots (Humanoids)*, Nov. 2012, pp. 734–740.

[15] O. E. Ramos, N. Mansard, and P. Soueres, "Whole-body motion integrating the capture point in the operational space inverse dynamics control", in *Humanoid Robots (Humanoids), 2014 14th IEEE-RAS International Conference on*, IEEE, 2014, pp. 707–712.

[16] A. Hof, M. Gazendam, and W. Sinke, "The condition for dynamic stability", *Journal of Biomechanics*, vol. 38, no. 1, pp. 1–8, 2005.

[17] M. B. Popovic, A. Goswami, and H. Herr, "Ground reference points in legged locomotion: Definitions, biological trajectories and control implications", *The International Journal of Robotics Research*, vol. 24, no. 12, pp. 1013–1032, 2005.

[18] T. Koolen, J. Smith, G. Thomas, S. Bertrand, J. Carff, N. Mertins, D. Stephen, P. Abeles, J. Englsberger, S. McCrory, J. Van Egmond, M. Griffioen, M. Floyd, S. Kobus, N. Manor, S. Alsheikh, D. Duran, L. Bunch, E. Morphis, L. Colasanto, K.-L. Ho Hoang, B. Layton, P. Neuhaus, M. Johnson, and J. Pratt, "Summary of team IHMC's virtual robotics challenge entry", in *Humanoid Robots (Humanoids), 13th IEEE-RAS International Conference on*, Oct. 2013.